Modelling surface radioactive, chemical and oil spills in the Strait of Gibraltar ☆

R. Periáñez *, A. Pascual-Granged

Dpto. Física Aplicada I, E.U. Ingeniería Técnica Agrícola, Universidad de Sevilla, Ctra, Utrera km 1,41013 Sevilla, Spain

Abstract

A model that simulates the dispersion of chemical/radioactive and oil spills in the Strait of Gibraltar has been developed. Water currents over the Strait have been obtained from a hydrodynamic model. Computed tides and residual currents have been compared with observations in the area. The dispersion model, based on a particle-tracking technique, is solved off-line. Standard tidal analysis, carried out over results provided by the hydrodynamic model, is applied to obtain currents at any time and position of the Strait. Specific processes for each contaminant (decay of radioactive material, oil evaporation and decomposition) are included and simulated by means of a stochastic method. A Monte Carlo method is applied for turbulent diffusion. The model can deal with instantaneous and continuous releases. MatLab graphic user interfaces have been developed to introduce input data and visualize simulation results. Some dispersion calculations have been carried out. In general, contaminants are flushed towards the east due to the residual currents. Nevertheless, dominant east winds tend to retain contamination in the Strait and to enhance mixing. This is also the case if the release occurs close to the coast, where currents are weaker than in the central part of the Strait.

Keywords: Strait of Gibraltar; Spill simulations; Hydrodynamic modelling; Particle tracking; Tides; Decision making

1. Introduction

Numerical models for simulating pollutant dispersion are nowadays being developed since they can be used for decision-making purposes after releases of contaminants into the marine environment. In particular, particle-tracking methods are well suited for problems in which high contamination gradients are involved, since they do not introduce numerical diffusion. Also, they can give very fast answers, specially if the hydrodynamic calculations are made off-line and tidal analysis and computed residuals are used to reconstruct water movements, which avoids the Courant–Friederichs–Lewy (CFL) stability limitations in the dispersion calculations. Thus, particle-tracking models are very useful predictive tools that can be used for assessing contamination after accidental or deliberate releases. Particle-tracking models have been used to simulate the dispersion of passive tracers (Stentchev and Korotenko, 2005; Harms et al., 2000; Gómez-Gesteira et al., 1999), radionuclides (Schonfeld, 1995; Periáñez and Elliott, 2002; Nakano and Povinec, 2003), oil spills

☆ Code available from server at http://www.iamg.org/CGEditor/index.htm.

*Corresponding author. Fax: +34 954486436.
E-mail address: rperianez@us.es (R. Periáñez).

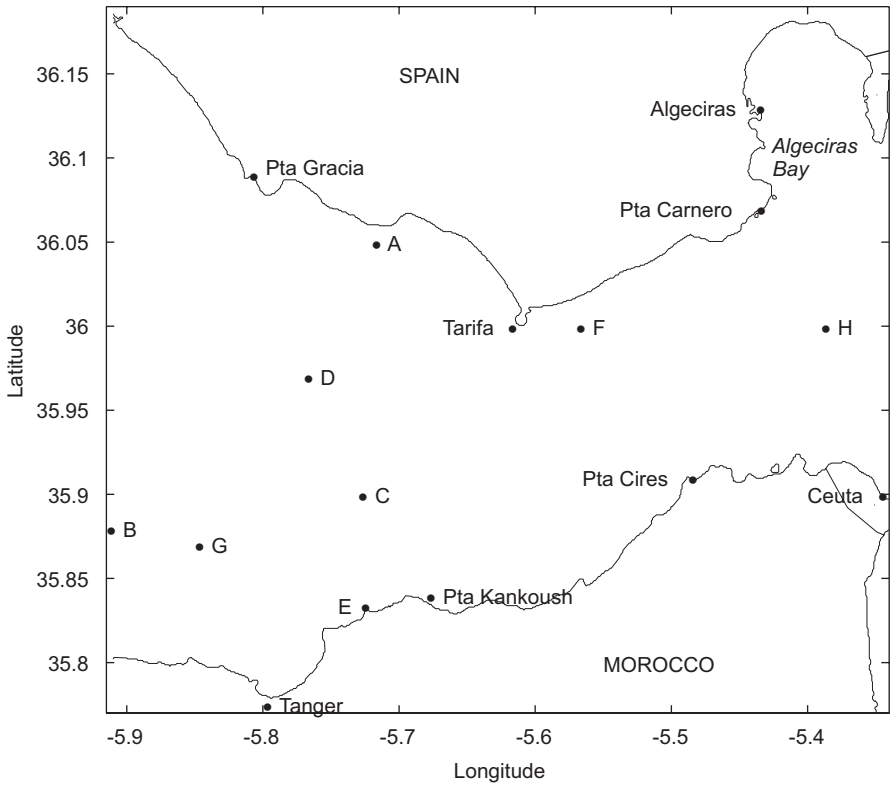

Fig. 1. Map of the Strait of Gibraltar showing some important towns and locations where tide amplitudes and currents have been compared with observations.

(Proctor et al., 1994a,b; Korotenko et al., 2004) and even contaminated milk (Elliott et al., 2001) in coastal waters.

The area of the Strait of Gibraltar has a high ecological value, being essential in marine and aerial migratory processes. As the only connection between the Mediterranean Sea and the Atlantic Ocean, marine turtles and mammals (dolphin, porpoise, sperm whale, killer whale) travel through the Strait. Also, the region has a high tourist interest, since many kilometers of sand beaches attract thousands of tourists each year. Finally, there are also some important towns. A release of contamination in the area as a consequence of an accident (or a deliberate release) can lead to significant ecological and economic impacts.

Shipping activities in the area of interest are very intense, again due to the fact that it is the only connection between the Atlantic and the Mediterranean. There is a traffic over 70,000 merchant vessels per year, 30% of them declaring hazardous cargos. Traffic of oil tankers is about 5000 vessels per year. Transit of nuclear submarines and of vessels transporting radioactive waste must also be considered. Only in the Strait of Gibraltar there are over 12,000 vessels (mostly passenger ferries) crossing per year between the north and south coasts. Fishing activities have to be included. Algeciras is the most important port in Spain (and number 25 in the world), with 61.7 Mt of cargo handled in 2004.[1] A map of the Strait may be seen in Fig. 1.

It is usual to have adverse meteorological conditions in the Strait, with more than 54% of days of moderate to poor visibility and 13% of days with persistent fog conditions. Winds must be added, with frequent east and west gales. East winds (*levantes*) blow an average of 165 days per year, predominantly from April to October, with an average speed of the order of 50 km/h. Maximum speed reaches 125 km/h. Gusts of winds can remain up to 7–10 days. West winds (*ponientes*) blow an average of 60 days per year, from November to March predominantly. Minimum and maximum speeds are 30 and 90 km/h. West winds are not as persistent as *levantes*, lasting for some 12–36 h.

[1]Autoridad Portuaria de la Bahía de Algeciras, 2006. External link http://www.apba.es (in English and Spanish).

The particular conditions in the area (intense traffic and adverse meteorology) make navigation difficult. Indeed, 81 accidents have occurred in the Strait in the last years,[2] with 14 collisions and 16 groundings. For instance, in 1990 there was a collision between the oil tanker Hesperus and the chemical tanker Sea Spirit. More recently, a ferry and a gas tanker collided off Ceuta.

The objective of this work consists of describing a rapid-response model developed to simulate the dispersion of radioactive, chemical or oil spills occurring in the Strait. A first approach was already described in Periáñez (2005a). Such model was named GIbraltar Strait PARticle-Tracking model (GISPART); however, its resolution was poor (2500 m) and it could not simulate oil spills. Thus, the model has been improved enhancing resolution (this was a must in a region of abrupt topography changes as the Strait), accounting for oil spills and, also, for variable wind fields (wind had to remain constant in the earlier model version). Finally, MatLab graphic user interfaces (GUIs) have been developed to allow an easier model–user interaction. This model can be used to support the decision-making process after a release of contamination in the area.

The hydrodynamic is solved in advance. A 2D depth-averaged barotropic model is used to obtain tidal currents in the region. Tidal and mean circulation are stored in files that will be read by the dispersion code to compute water current at any time and position. Dispersion is solved using a particle-tracking method. Thus, the spill is simulated by a number of particles, each of them equivalent to a number of units (for instance, kg or Bq), whose paths are followed in time. Specific processes for each contaminant are included in the model using stochastic techniques (radioactive decay, oil evaporation and biodegradation). A Monte Carlo random-walk method is used to calculate turbulent diffusion. Contaminant concentrations may be obtained at the desired time from the density of particles per water volume unit.

The hydrodynamic and dispersion models are described in the following section. Next, results obtained with the hydrodynamic model are presented. In particular, computed tides and mean circulation are compared with observations in the Strait. Then some examples of dispersion calculations are discussed. These calculations have been carried out for chemical contaminants and oil spills and under different wind conditions.

[2]Nav42, 1998. Report to the Maritime Safety Committee. International Maritime Organization. External link http://www.navcen.uscg.gov/marcomms/imo/document.htm

2. Model description

2.1. Hydrodynamic model

An important feature of the tidal flow in the Strait is that it can be considered, as a first approach, as barotropic. Indeed, 93% of the current velocity variance in the semidiurnal band has a barotropic character in the Strait (Mañanes et al., 1998). Tsimplis and Bryden (2000) have pointed out that tidal currents are barotropic and larger than the mean inflow or outflow. The semidiurnal tide dominates acoustic Doppler current profiler (ADCP) records in the Strait, obscuring the expected two-layer character of the mean flow. The tidal signal is so strong that it reverses the currents near the bottom for a part of each tidal cycle. As a consequence, 2D depth-averaged models have already been applied to simulate surface tides in the Strait (Tejedor et al., 1999). Tsimplis et al. (1995) have even used a 2D barotropic model for simulating tides in the whole Mediterranean Sea. Also, pollutants considered in this work are released at the sea surface and remain close to the surface after the typical simulated times (several days). Thus, the use of a 2D depth-averaged barotropic model is justified to obtain surface currents.

The depth-averaged hydrodynamic equations may be written as (Periáñez, 2005b)

$$\frac{\partial z}{\partial t}+\frac{\partial}{\partial x}(Hu)+\frac{\partial}{\partial y}(Hv)=0, \tag{1}$$

$$\frac{\partial u}{\partial t}+u\frac{\partial u}{\partial x}+v\frac{\partial u}{\partial y}+g\frac{\partial z}{\partial x}-\Omega v+\frac{\tau_u}{\rho H} = A\left(\frac{\partial^2 u}{\partial x^2}+\frac{\partial^2 u}{\partial y^2}\right), \tag{2}$$

$$\frac{\partial v}{\partial t}+u\frac{\partial v}{\partial x}+v\frac{\partial v}{\partial y}+g\frac{\partial z}{\partial y}+\Omega u+\frac{\tau_v}{\rho H} = A\left(\frac{\partial^2 v}{\partial x^2}+\frac{\partial^2 v}{\partial y^2}\right), \tag{3}$$

where u and v are the depth-averaged water velocities along the x- and y-axis, D is the depth of water below the mean sea level, z is the displacement of the water surface above the mean sea level measured upwards, $H = D + z$ is the total

water depth, Ω is the Coriolis parameter ($\Omega = 2w \sin\beta$, where w is the Earth rotational angular velocity and β is latitude), g is acceleration due to gravity, ρ is water density and A is the horizontal eddy viscosity. τ_u and τ_v are friction stresses that have been written in terms of a quadratic law:

$$\tau_u = k\rho u\sqrt{u^2+v^2},$$
$$\tau_v = k\rho v\sqrt{u^2+v^2}, \quad (4)$$

where k is the bed friction coefficient.

The solution of these equations provides the water currents at each point in the model domain and for each time step. Currents are treated through standard tidal analysis (Pugh, 1987, Chapter 4) and tidal constants are stored in files that will be read by the dispersion code to calculate the advective transport of particles. The model includes the two main tidal constituents, M_2 and S_2. Thus, the hydrodynamic equations are solved for each constituent and tidal analysis is also carried out for each constituent separately. A residual transport cannot be produced by the pure harmonic currents given by the tidal analysis, thus tidal residuals have been calculated as well as explained below.

Some open boundary conditions must be provided to solve the hydrodynamic equations. Surface elevations are prescribed as periodic functions of time along the open boundaries of the computational domain (Fig. 2). These elevations are obtained from observations (Candela et al., 1990; García-Lafuente, 1986). A radiation condition is applied to the water velocity component that is normal to the open boundary:

$$\frac{\partial\phi}{\partial t} = c\frac{\partial\phi}{\partial n}, \quad (5)$$

where ϕ is the current component normal to the boundary, in the direction n, and c is a phase speed calculated as in Jensen (1998). Water flux across a land boundary is set to zero as usual.

The hydrodynamic equations are solved using an explicit finite difference scheme on a grid with resolution $\Delta x = \Delta y = 1000$ m. The scheme is described in detail in Flather and Heaps (1975) and Periáñez (2005b). Time step, limited by the CFL condition, is $\Delta t = 5$ s. Once a stable periodic solution is achieved, tidal analysis is carried out to determine tidal constants that are used by the particle-tracking code. Tidal residual transports are also calculated. This is done for the M_2 and S_2 tides

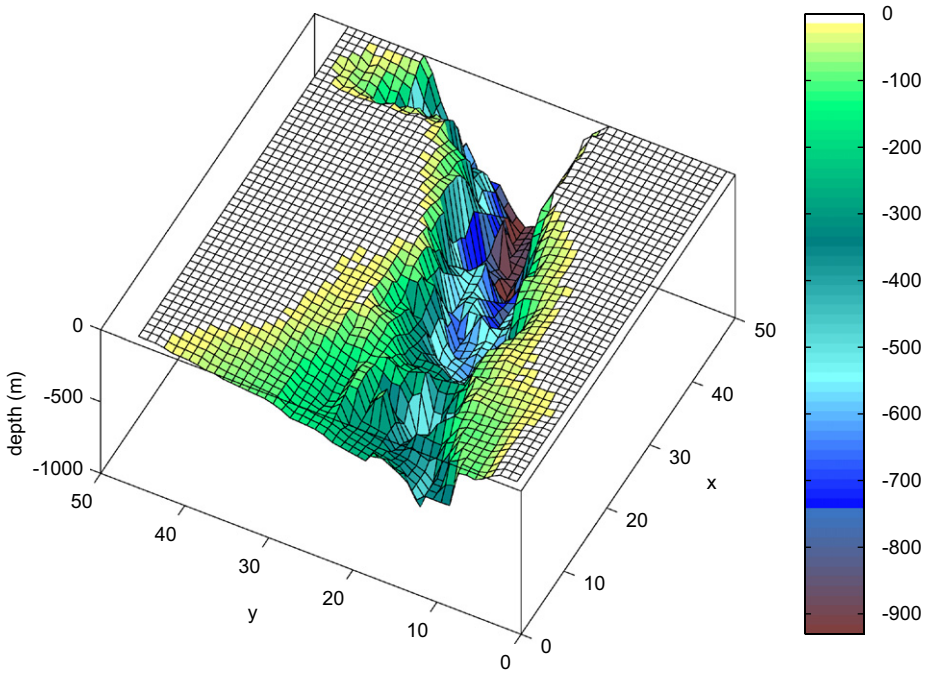

Fig. 2. Computational domain showing topography of the Strait. Each unit in x- and y-axis is grid cell number (thus equal to 1000 m). North is in the y direction. Units in the color scale are m.

separately. Tidal residuals for each constituent are calculated from the equation

$$\vec{q}_r = \frac{\langle H\vec{q}_t \rangle}{\langle H \rangle} \tag{6}$$

which corresponds to the Eulerian residual transport velocity (Delhez, 1996). In this equation $\langle\rangle$ is the time averaging operator, $\vec{q}_r$ is the tidal residual and $\vec{q}_t$ is the instantaneous tidal current. In addition, the mean current due to geostrophic flow is calculated from an additional run of the hydrodynamic model. In this run constant values of the sea surface elevation along the two open boundaries of the domain are specified (Sannino et al., 2004). The total mean current is obtained adding the tidal residuals of the M_2 and S_2 constituents plus the mean geostrophic flow. Current $\vec{q}$ at any time and position in the Strait is obtained adding this total mean current and the instantaneous tidal currents at the corresponding point. This is the current value used in the dispersion calculations.

The computational grid extends from 35.77°N to 36.19°N and from 5.91°W to 5.34°W. Water depths were introduced from a bathymetric chart (Fig. 2).

2.2. Dispersion model

Advection is computed solving for each particle the equation

$$\frac{\mathrm{d}\vec{r}}{\mathrm{d}t} = \vec{q}, \tag{7}$$

where $\vec{r}$ is the position vector of the particle and $\vec{q}$ is the current vector solved in components u and v.

The particle-tracking model is 3D, but the hydrodynamic calculations provide depth-averaged currents. In the main body of water above the logarithmic layer, the flow gradually increases in a manner which may be represented as (Pugh, 1987)

$$u_{z'} = u_s \left(\frac{D - z'}{D} \right)^{1/m}, \tag{8}$$

where $u_{z'}$ is the current speed at a level z' below the sea surface and u_s is the surface flow. From observations, it has been deduced that m ranges between 5 and 7. The surface current can be deduced from the depth-averaged one (Pugh, 1987):

$$u_s = \frac{m+1}{m}\overline{u}, \tag{9}$$

where $\overline{u}$ is the depth-averaged current. Thus, components u and v of the current at any depth can be obtained from their depth-averaged values (provided by the hydrodynamic model) applying Eqs. (8) and (9). This current profile has already been used (Riddle, 1998) in particle-tracking dispersion models.

Wind is typically included in particle-tracking models assuming that the surface wind-induced current is 3% of the wind speed measured 10 m above the sea surface (Proctor et al., 1994a; Pugh, 1987). This current decreases logarithmically to zero at a depth z_1. This depth is assumed to be 20 m (Elliott, 1986). The wind-induced current at any depth z' below the surface is written as (Pugh, 1987)

$$u_{z'} = \begin{cases} u_0 - \frac{u^*}{\kappa} \ln\left(\frac{z'}{z_0}\right) & \text{if } z' < z_1, \\ 0 & \text{if } z' \geqslant z_1, \end{cases} \tag{10}$$

where u_0 is the surface wind-induced current, $\kappa = 0.4$ is the von Karman constant, u^* is a friction velocity and z_0 is the sea surface roughness length, which has values between 0.5 and 1.5 mm. It has been obtained (Pugh, 1987) that the friction velocity can be estimated as

$$u^* = 0.0012W \tag{11}$$

for a wide range of conditions, where W is wind speed 10 m above the sea surface. From these equations, the wind effect on the advection of particles can be calculated. Of course, the current profile is solved in the u and v components. It may be noted that wind is not included in the hydrodynamic calculations, but only in dispersion. This is the standard approach in rapid-response models, which require current fields computed in advance so that computation time is not drastically increased.

Table 1
Information required by the model to be introduced by user

Release point coordinates
Select instantaneous/continuous release option
Wind data file
Release date (day, month, year)
Release time, UTC (hours, minutes)
Residual current modulator
Simulation time (days)
Magnitude of the release in the corresponding units[a]
Contaminant decay constant (radioactive)
Oil spill additional information:
Oil density
Droplet minimum and maximum sizes
e-Folding times (evaporation and decomposition)

[a] In case of a continuous release, release rate is assumed to be constant along the duration of the accident.

The 3D diffusion is simulated using a random-walk (Monte Carlo) method. It has been shown (Proctor et al., 1994a) that it is a simulator of Fickian diffusion provided that the maximum size of the horizontal step given by the particle, D_h, is

$$D_h = \sqrt{12 K_h \Delta t} \tag{12}$$

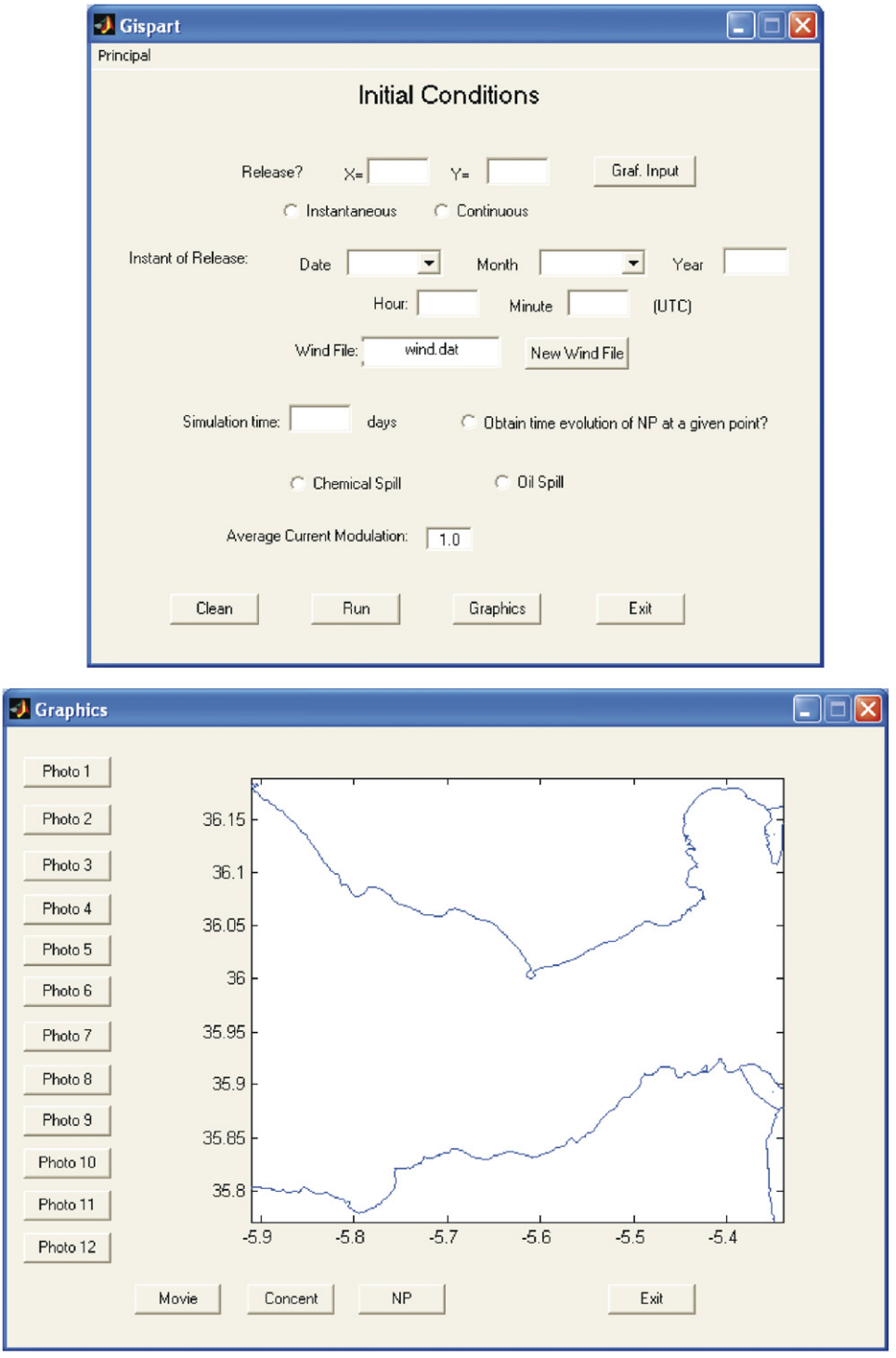

Fig. 3. Main (up) and output (down) GUIs.

in the direction $\theta = 2\pi RAN$, where RAN is a random number between 0 and 1. This equation gives the maximum size of the step. In practice, it is multiplied by RAN to obtain the real size at a given time and for a given particle. Similarly, the maximum size of the vertical step is

$$D_v = \sqrt{2K_v\Delta t} \tag{13}$$

given either towards the sea surface or the sea bottom. K_h and K_v are the horizontal and vertical diffusion coefficients, respectively.

Radioactive decay can be treated using a stochastic method if it is assumed that the probability p of removal of a particle at each time step is

$$p = 1 - \mathrm{e}^{-\lambda\Delta t}, \tag{14}$$

where λ is the radioactive decay constant. In practice, a random number is generated for each particle at each time step. If $RAN \leqslant p$ then the particle is removed from the computation. Obviously, in the case of a stable chemical pollutant $\lambda = 0$.

Some specific processes for oil have to be included. In addition to advection and 3D diffusion, droplets have a size distribution so that larger ones tend to remain in the water surface and move in the direction of wind. Smaller droplets mix downwards because of turbulence and shear diffusion results in a patch elongated in the current direction. The model also includes the effects of surface evaporation of oil and decomposition within the water column (for instance, because of biodegradation).

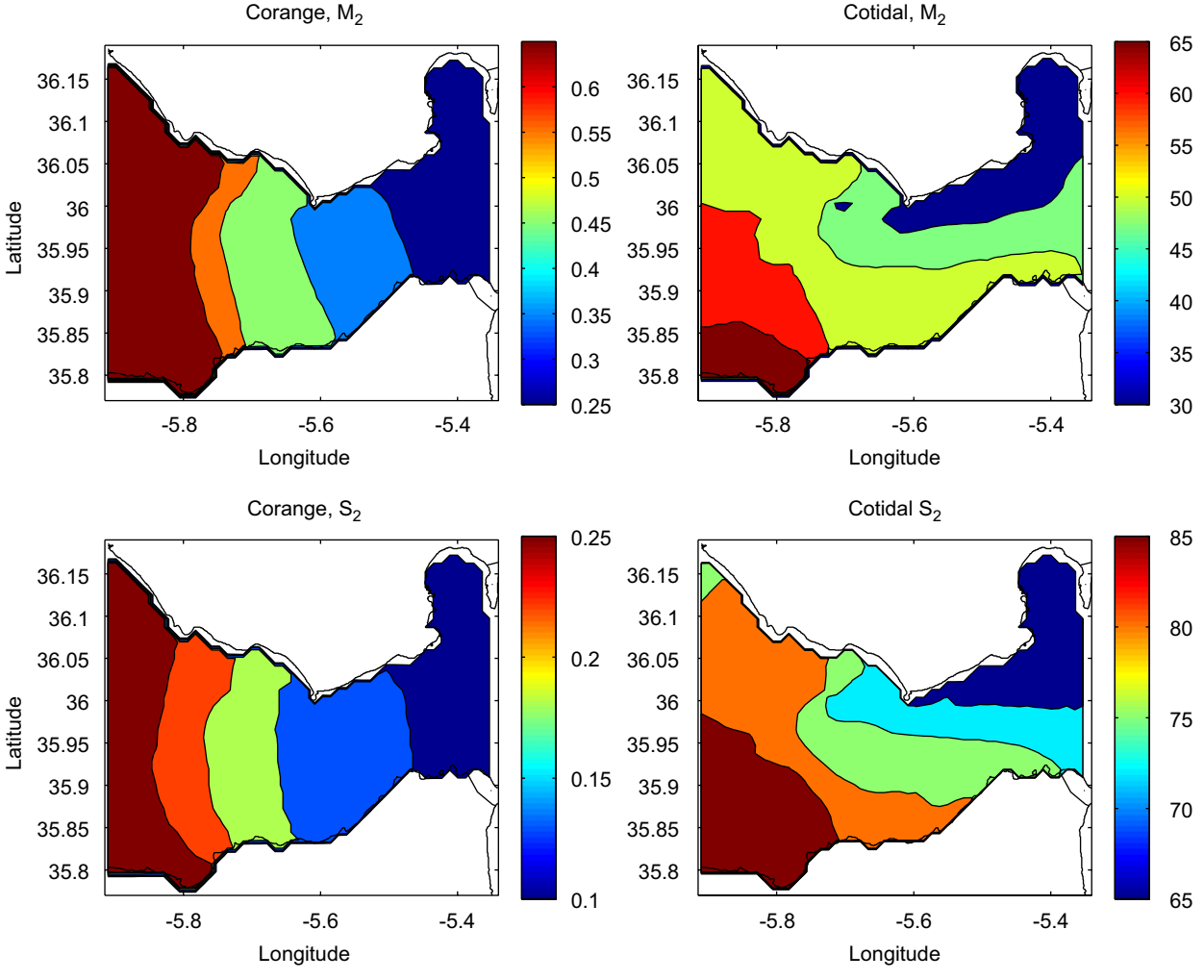

Fig. 4. Computed corange and cotidal charts for M_2 (up) and S_2 (down) tides. Amplitudes are given in m and phases in degrees.

The buoyancy force depends on the density and size of droplets. The vertical velocity, w, can be described as (Proctor et al., 1994a; Korotenko et al., 2004)

$$w = \frac{gd^2(1-\rho_0/\rho)}{18\nu} \tag{15}$$

for small droplets with diameter $d \leqslant d_c$ (laminar motion). In this equation ρ and ρ_0 are the densities of water and oil, respectively, and ν is the water kinematic viscosity. For large droplets with $d > d_c$ (turbulent motion) the vertical velocity is

$$w = \left(\tfrac{8}{3} g d(1-\rho_0/\rho)\right)^{1/2}. \tag{16}$$

The critical diameter, d_c, is given by the expression

$$d_c = \frac{9.52\nu^{2/3}}{g^{1/3}(1-\rho_0/\rho)^{1/3}} \tag{17}$$

that is deduced matching the Reynolds numbers at which the transition from laminar to turbulent flow occurs.

The diameter of each oil droplet in the simulation is assigned randomly between a minimum and maximum diameter, $d_{min} - d_{max}$.

The effects of oil evaporation and decomposition are treated in a similar way as radioactive decay. Thus, the probability of removal of particle in a time step is given by Eq. (14). The decay constant is related to the e-folding time by $\lambda = 1/T_e$. Different e-folding times are used for evaporation, T_{ev}, and decomposition, T_{de}. Additionally, only particles within a depth $z_{ev} = 0.25$ m below the surface can be evaporated, whereas droplets at any depth can experience decomposition (Proctor et al., 1994a). If during a computation an oil droplet reaches the coastline, it is considered *beached*. Thus, the droplet stays in the coast without moving any more.

Both instantaneous and continuous releases can be simulated. From the total amount of pollutant discharged, concentration maps can be obtained by counting the density of particles per water volume unit. Date and time of the discharge (and duration in the case of continuous releases) must be specified since the fate of the release will depend on the tidal state when it took place. Thus, the appropriate phase of each tidal constituent at $t = 0$ must be specified. The values used in this model correspond to the origin of time being January 1, 2003, at 0:15 h Greenwich time.

The adsorption of pollutants by suspended and bottom sediments can also be simulated with a particle-tracking model (Periáñez and Elliott, 2002). However, these processes are neglected in the present study since suspended matter concentrations are very low in the Strait, typically 0.1–0.5 mg/L (León-Vintró et al., 1999). Also, average depth is 350 m (reaching 900 m in the eastern part) and, as a consequence, interactions of pollutants with bed sediments can be neglected as well.

While there is no stability criterion equivalent to the CFL condition in the particle-tracking calculations, it is wise to ensure that each particle does not move through a distance that exceeds the grid spacing during each time step. This was satisfied using a time step of 100 s.

2.3. Graphical user interfaces

MatLab GUIs have been created to allow an easy use of the model, although computation codes are written in FORTRAN. The first, main, GUI is shown in Fig. 3. It is used to introduce all the information required by the model, that is summarized

Table 2
Observed and computed amplitudes (A, cm) and phases (g, deg) of tidal elevations at some locations indicated in Fig. 1

Station	M_2				S_2			
	A_{obs}	g_{obs}	A_{comp}	g_{comp}	A_{obs}	g_{obs}	A_{comp}	g_{comp}
Pta Gracia	64.9	49	71.9	59	22.3	74	24.9	82
D	60.1	52	57.5	53	22.5	74	21.4	79
C	54.0	62	54.1	54	21.1	83	20.0	82
A	52.3	48	57.5	54	18.5	73	20.9	79
E	57.1	67	59.8	60	20.6	92	21.4	87
B	78.5	56	78.5	64	29.0	82	27.0	89
Pta Kankoush	51.8	69	51.3	54	20.1	90	19.1	83
Tarifa	41.5	57	42.9	46	14.2	85	16.6	73
F	44.4	48	39.8	45	16.1	74	15.4	72
Pta Cires	36.4	47	37.8	52	14.1	74	14.0	79
Algeciras	31.0	48	29.1	47	11.1	74	11.0	72
Pta Carnero	31.1	48	29.1	46	11.5	71	11.0	71
Ceuta	29.7	50	29.6	52	11.4	76	10.9	74

Table 3
Observed and computed amplitudes (q, m/s) and phases (g, deg) of M_2 and S_2 barotropic tidal velocities at three locations in Fig. 1

Station	M_2				S_2			
	q_{obs}	g_{obs}	q_{comp}	g_{comp}	q_{obs}	g_{obs}	q_{comp}	g_{comp}
C	0.91	147	0.94	126	0.31	171	0.37	177
H	0.25	160	0.31	115	0.12	178	0.13	154
G	0.65	157	0.62	129	0.23	182	0.25	172

in Table 1. The release point and the point where the time evolution of the number of particles is obtained (if the option is selected) can be introduced as geographic coordinates or, alternatively, from another GUI simply clicking at the point with the mouse. Wind data can be directly introduced from this GUI or included into a file externally edited. The mean current in the Strait is also affected by

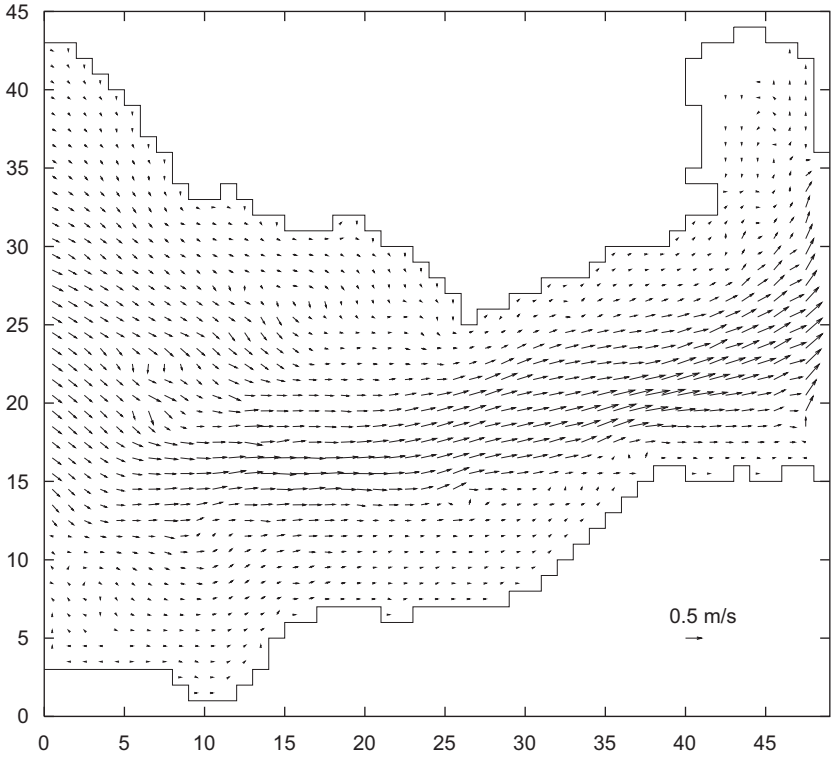

Fig. 5. Computed residual currents in the Strait. Each unit in x- and y-axis is grid cell number (thus equal to 1000 m).

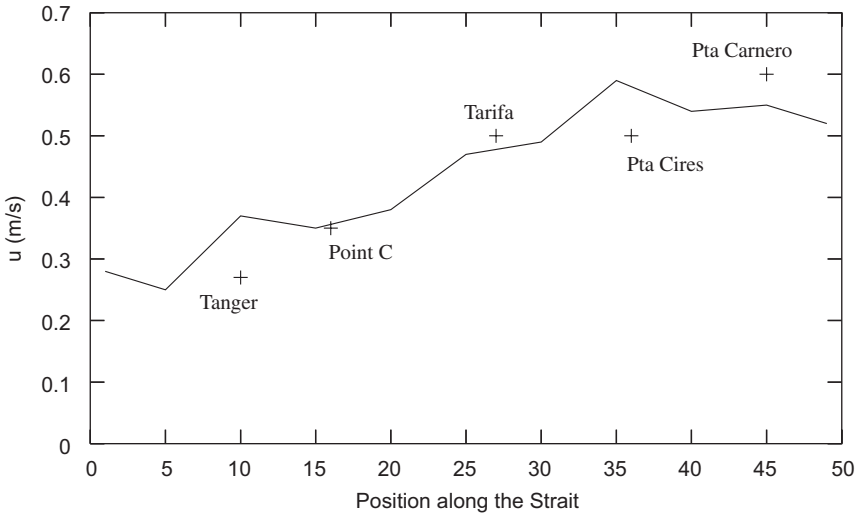

Fig. 6. Computed u component of mean current along axis of the Strait (line). Points correspond to results of Sannino et al. (2004). Names (see Fig. 1) help to identify position.

other factors as, for instance, atmospheric pressure differences between the Atlantic and the western Mediterranean, and thus presents some variability. Thus, a factor that acts as a modulator of the residual current amplitude must be introduced. If 1 is used, the residual current for the mean water inflow through the Strait is used in the calculations. These mean currents may be amplified or reduced by specifying values for the modulator larger or smaller than 1, respectively.

It is worth commenting that it is difficult to provide a value for this modulator: let us imagine that an accident occurs just now. How do we run the model? In other words: Which is the water inflow through the Strait just now? Presently, it is not possible to have an answer. Thus, it is recommended to carry out calculations under the most probable conditions in a first guess (using the mean current, with a modulator equal to 1). Additional simulations may then be carried out using other current modulators to increase and reduce water velocities. This method will, at least, allow to estimate if there is any chance that a given sensible point (a coastal town, for instance) is affected by contamination. Given the short running times of the model (12 s per day of simulation on a Pentium 4 PC in the case of an instantaneous release), this is not a problem. This procedure has already been suggested for a radioactive spill model recently developed for the Alborán Sea (Periáñez, 2006).

If the graphic button is pressed, the output GUI is opened (also in Fig. 3). Twelve snapshots at constant

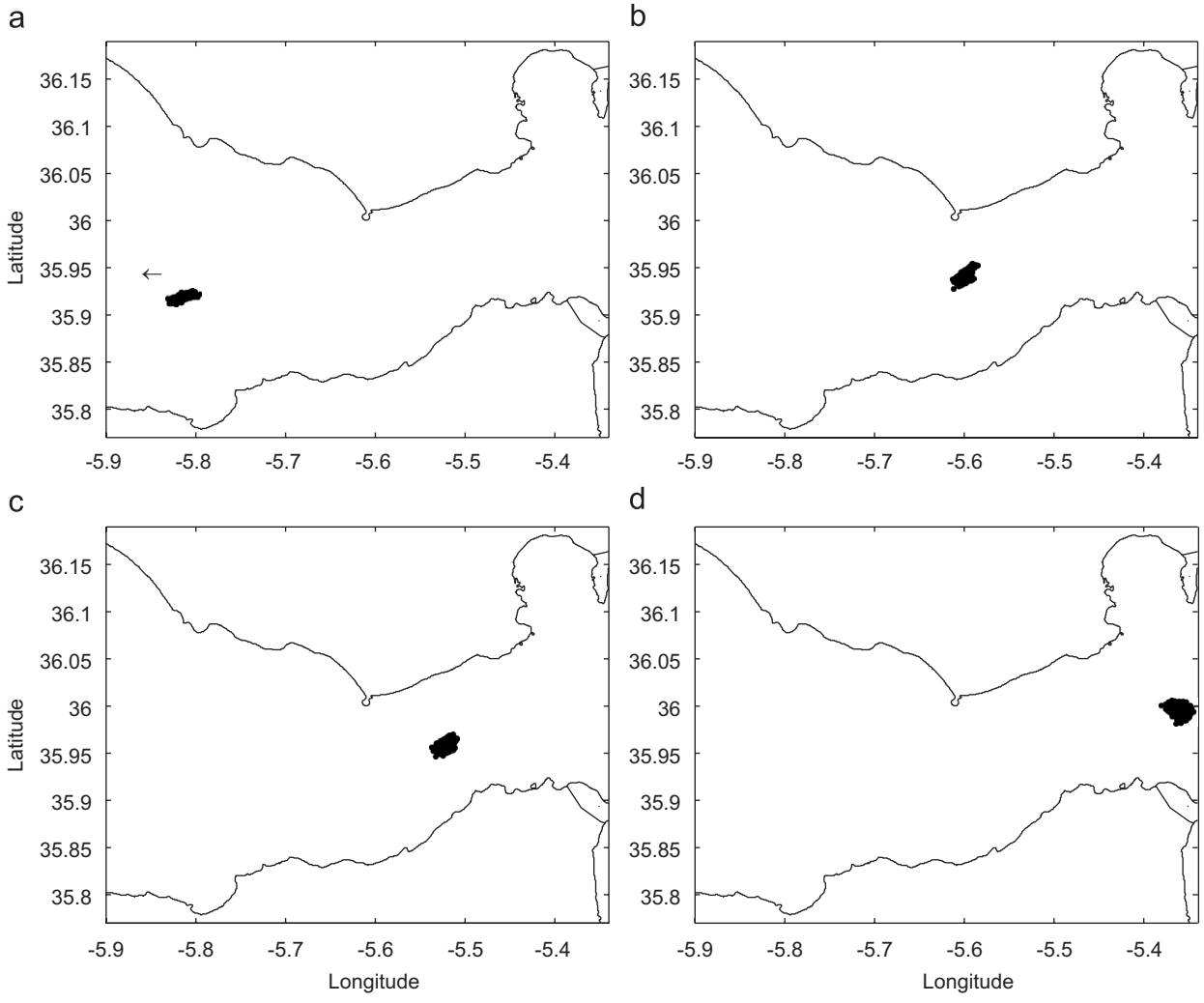

Fig. 7. Position of particles at 8 (a), 16 (b), 20 (c) and 24 (d) h after an instantaneous release at the arrow position.

intervals during the simulation may be plotted to show the evolution of the contamination patch over time. Photographs may be seen one by one or as a movie. Another graphic consists of a map of the final pollutant concentration over the Strait (concent button) computed from the density of particles per water volume unit. If the option was selected, the time evolution of the number of particles at the selected point may be finally seen (NP button).

3. Results and discussion

3.1. Hydrodynamics

After a calibration process, the bed friction coefficient was fixed as $k = 0.070$ and the horizontal eddy viscosity as $A = 10\,\mathrm{m}^2/\mathrm{s}$. In general, good agreement between model results and observations is obtained with these values. Computed tidal charts for the M_2 and S_2 tides are presented in Fig. 4. They are in agreement with those previously computed by Tejedor et al. (1999) QJ;and with the observations in Candela et al. (1990). They show an amplitude reduction in a factor 2 approximately along the Strait in both tides, and essentially constant amplitudes across the Strait. Cotidal lines are essentially oriented in a northwest–southeast direction. Good quantitative agreement is also obtained. Observed and computed amplitudes and phases of both tides at several locations in the Strait, shown in Fig. 1, are given in Table 2.

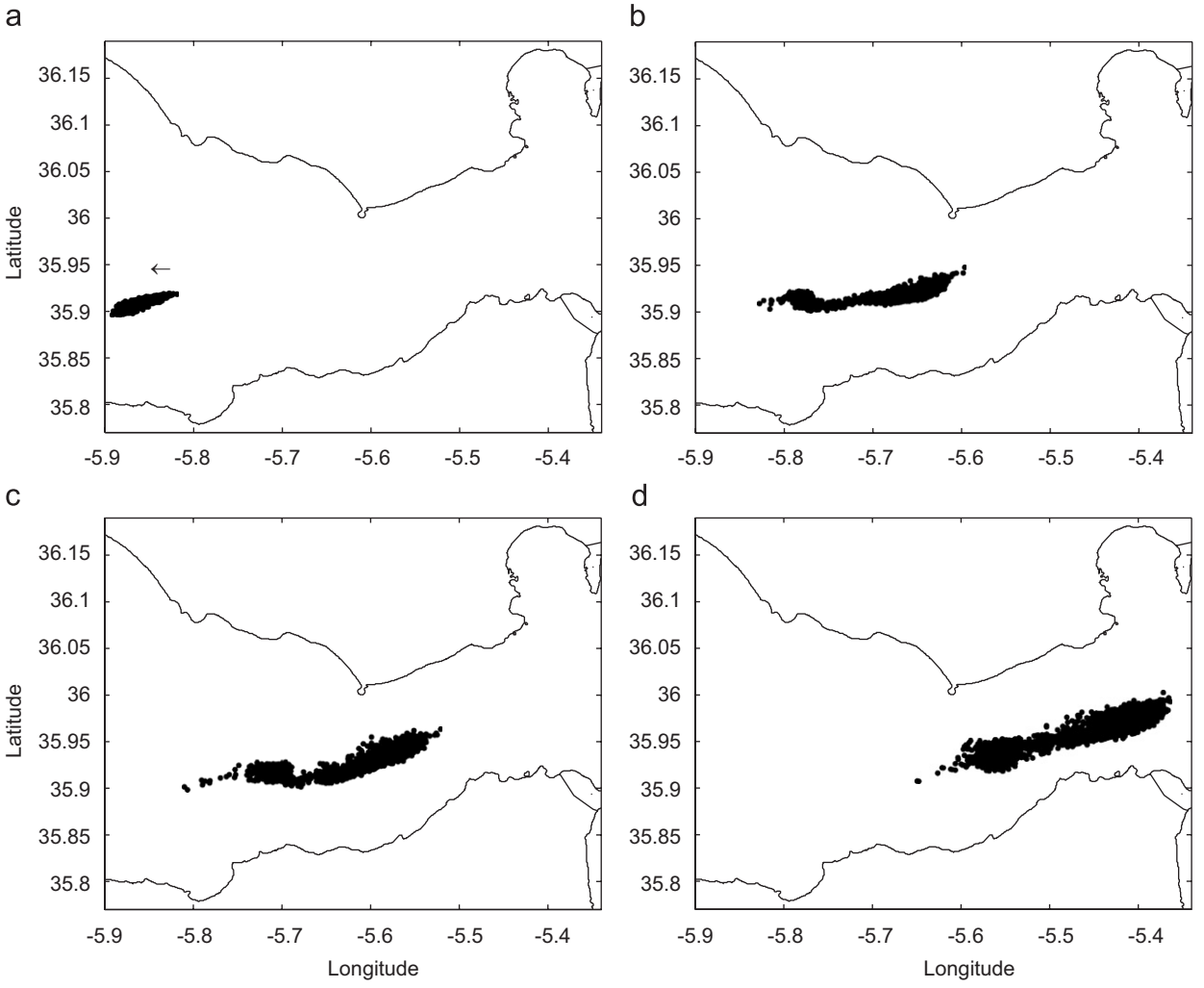

Fig. 8. Position of particles at 8 (a), 16 (b), 20 (c) and 24 (d) h after an instantaneous release at the arrow position. Wind from the east, speed 15 m/s.

A comparison between computed and barotropic current amplitudes and phases deduced from measurements (Mañanes et al., 1998) in the Strait can be seen in Table 3. The agreement in currents is not so good as in the case of tidal elevations, specially for the M_2 tide. However, the difficulty in appropriately defining the barotropic current has already been commented by Tejedor et al. (1999) when they compared barotropic currents predicted by their model with those derived from observations in the Strait.

The computed mean currents in the Strait are presented in Fig. 5. It can be seen that maximum currents are obtained in the central part of the Strait, and they are directed along its axis. The magnitude of the mean currents increases as going to the east. The u component (along strait) of the mean current magnitude along the axis of the Strait is presented in Fig. 6 together with the earlier calculations of Sannino et al. (2004). It may be seen that both models give very similar residual currents along the Strait.

Thus, it seems that, generally speaking, the present model gives a representation of the Strait circulation that is realistic enough to implement on it the particle-tracking dispersion code.

3.2. Dispersion model

Ideally, results from the dispersion model should be compared with observations after a real accident in the Strait. However, there are no data until now to carry out this work. Thus, we could only simulate some hypothetical accidents simply to show that results are logical and consistent.

Values for the diffusion coefficients have to be provided. The horizontal diffusion coefficient depends on the horizontal grid spacing. Following Dick and Schonfeld (1996):

$$K_h = 0.2055 \times 10^{-3} \Delta x^{1.15}. \tag{18}$$

The present grid resolution gives $K_h = 0.58\,\mathrm{m}^2/\mathrm{s}$. For the vertical diffusion coefficient a typical value of $0.001\,\mathrm{m}^2/\mathrm{s}$ is used (Elliott et al., 2001; Schonfeld, 1995; Dick and Schonfeld, 1996; Elliott, 1999).

A first numerical experiment consisted of simulating an instantaneous release of a chemical stable pollutant at coordinates -5.86° longitude, 35.95° latitude, that corresponds to grid cell (5,20). Date and time of the release are January 1, 2006, 0:00 h UTC (there is not any reason for selecting this instant of time, it is just an example). The total amount released was supposed to be 1.0×10^{12}

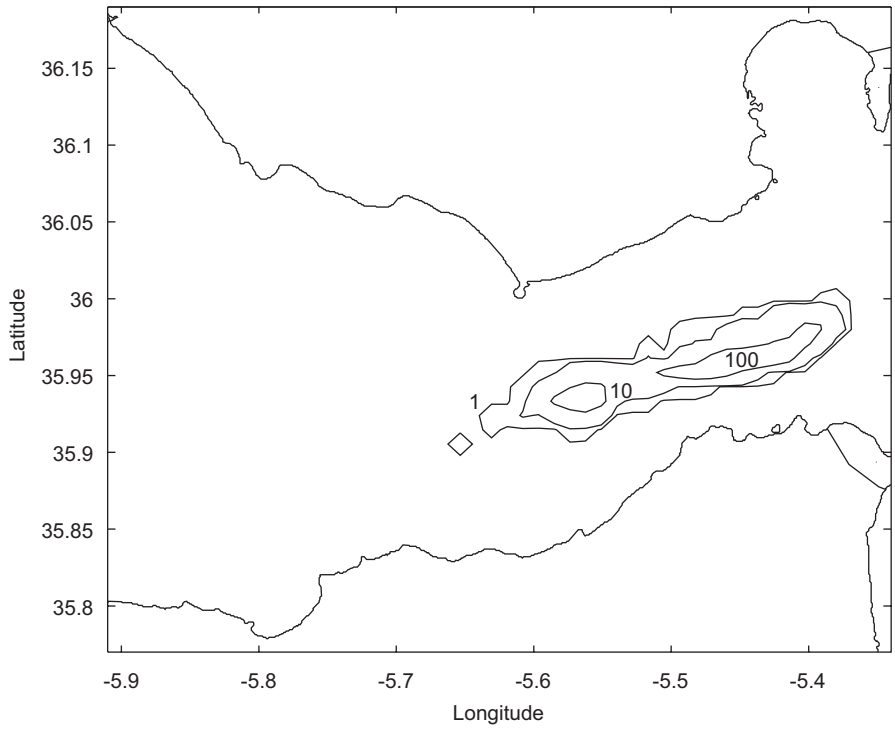

Fig. 9. Computed contaminant concentrations (units/m^3) for experiment in Fig. 8, 24 h after release.

units. No wind is assumed. The position of the contamination patch at 8, 16, 20 and 24 h after the release can be seen in Fig. 7. Although it cannot be appreciated in the figure, the patch oscillates forward and backward because of tides. Nevertheless, there is a net transport directed to the Mediterranean caused by the residual current. The mean transit velocity along the Strait, 0.50 m/s, results (43 km in 1 day) in excellent agreement with the typical inflow velocity given by Echevarría et al. (2002). Winds may vary this transport velocity, thus the time-scale of interest ranges from several hours to several days (Echevarría et al., 2002) and the spatial and temporal resolution of the model seems appropriate for solving dispersion processes in the Strait of Gibraltar.

The same experiment has been repeated but considering a constant 15 m/s wind from the east (*levante* wind is the most frequent in the Strait). Results are shown in Fig. 8, that may compared with Fig. 7. It can be clearly observed that east winds tend to retain contaminants in the Strait for a longer time. Also, shear dispersion is enhanced and, as a consequence, the size of the patch increases in the wind direction. The result is that, after 1 day, the contamination patch extends over some 20 km. As another example of the results that may be obtained from the model, the map of contaminant concentrations over the Strait for this experiment, from the density of particles per water volume unit, is presented in Fig. 9.

Winds from the west, in the same direction as the mean current, produce a faster contaminant flush-off from the Strait.

Generally speaking, a contamination patch released in the central region of the Strait will be

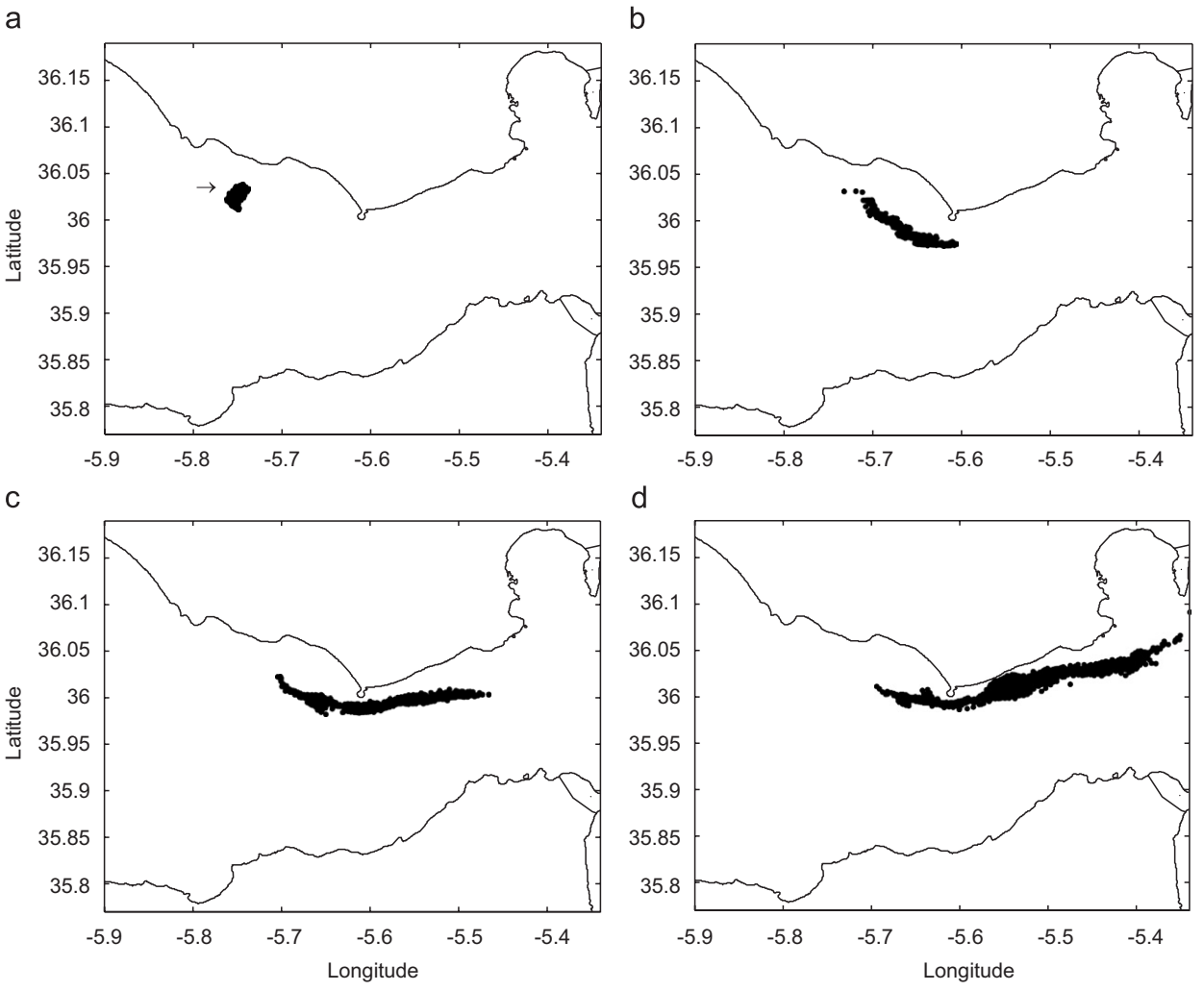

Fig. 10. Position of particles at 8 (a), 24 (b), 36 (c) and 48 (d) h after an instantaneous release at the arrow position.

flushed out of the model domain after a few days (depending on wind conditions). However, these initial days are the most relevant from a decision-making point of view, since pollutant concentrations are higher and, as a consequence, risk (for instance, dose in the case of a radioactive release) is also higher. Nevertheless, if the accident occurs close to the shoreline, the time required to flush out contaminants increases. This may be seen with the example presented in Fig. 10, where the instantaneous release occurs close to the Spanish shore: -5.78° longitude, 36.04° latitude. Residual currents are weaker along the shores of the Strait (Fig. 5), thus contaminants stay in the area for a longer time (in this case the patch is still in the Strait after 48 h). Forward and backward oscillations of the patch are now more evident, although the full sequence of images is not shown. Also, the patch increases its size in the direction of the current because of the strong horizontal current shear. Finally, it may be seen that the Spanish coast is affected by contamination. As an example, the time evolution of the pollutant concentration south of Tarifa (coordinates -5.61° longitude, 35.99° latitude) is shown in Fig. 11. It may be seen that contamination arrives this point 32.3 h after the accident, and that the maximum concentration (755 units/m^3) occurs 35.6 h after the release. The effect of tidal oscillations may be appreciated as well in Fig. 11.

The situation is similar if the accident occurs close to the coast of Morocco: contaminants are retained for a longer time in the Strait, the patch increases its size in the longitudinal direction and the coast is affected by contamination.

Some examples of model results in the case of oil spills are presented now. Values for the parameters required by the oil spill model must be set first. Oil density typically ranges from 660 kg/m^3 in the case of paraffin to 1200 kg/m^3 in the case of aromatic (poly-cyclic) and naphtheno-aromatic oils (Korotenko et al., 2004). A density equal to 900 kg/m^3 will be used in the simulations, that is between the value 870 kg/m^3 used in some calculations carried out for the Arabian Gulf spills of 1991 (Proctor et al., 1994a), and the value 950 kg/m^3 used in some hypothetical oil spill simulations for the Irish Sea (Elliott, 2004).

The oil droplet size is assumed to be in the range $60-600\,\mu m$, that are typical values (Proctor et al., 1994a; Elliott, 2004; Korotenko et al., 2004). The same values for the oil e-folding times as in Proctor et al. (1994a) have been used: 25 and 250 h for evaporation and decomposition, respectively.

An example of results is presented in Fig. 12. The oil spill is supposed to occur close to the coast, at a

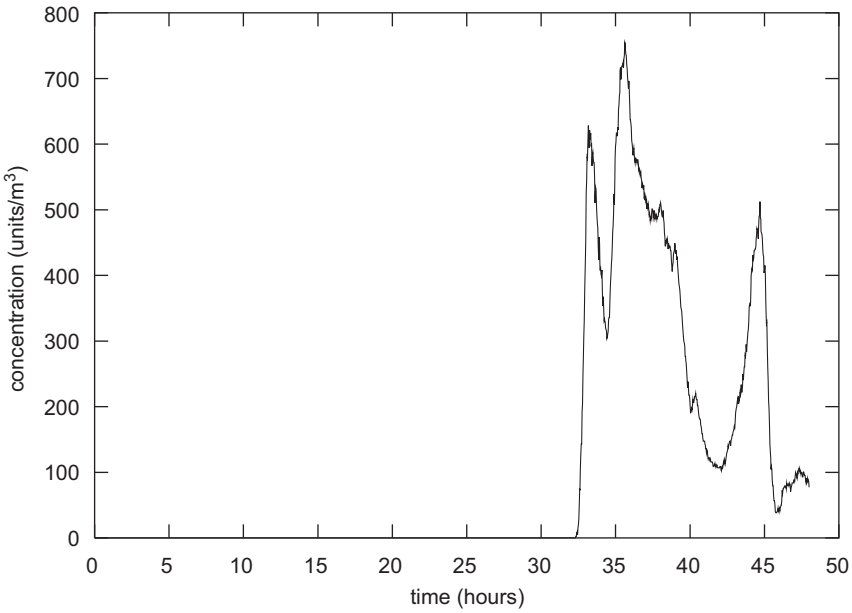

Fig. 11. Time evolution of pollutant concentration at position -5.61° longitude, 35.99° latitude (south of Tarifa) for experiment shown in Fig. 10.

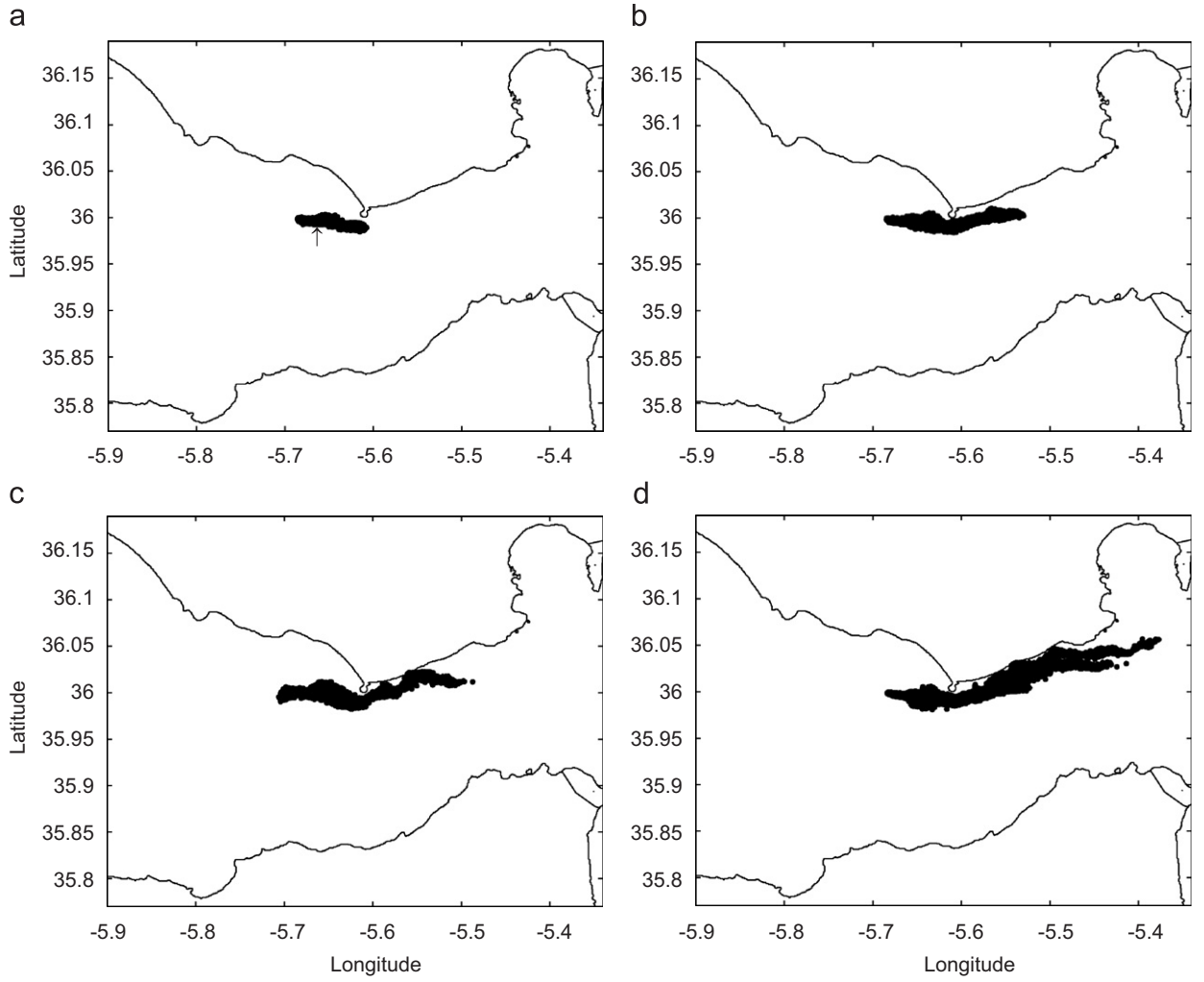

Fig. 12. Position of particles at 12 (a), 24 (b), 32 (c) and 48 (d) h during a continuous oil release at the arrow position.

point with coordinates -5.68° longitude, 36.00° latitude [cell (20,25)]. This example also illustrates how continuous releases are simulated. The dispersion of the continuous release is simulated over 2 days. Initial time and date are the same as in the examples above and no wind is considered. A total amount of 1.0×10^{12} units of oil is released, at a constant rate. It may be seen in Fig. 12 that a plume of oil is obtained from the release point to the east. This plume contaminates the coast of Spain. Indeed, particles beached after 36 and 48 h are shown in Fig. 13. Some areas of the coast, between Tarifa and Pta Carnero, are affected by oil. In this simulation 43,200 particles are released in total, at a rate of 25 new particles per time step. Since the total amount released is 1.0×10^{12} units, this implies 2.3×10^{7} units/particle. At the end of the simulation 329 particles are beached and 20,705 remain in water (the remaining have decayed), thus 7.6×10^{9} units of oil has reached the coast.

Finally, an accident occurring close to Algeciras port, where an oil refinery is located, has been simulated. Due to the weak tidal and residual currents in Algeciras Bay, a spill remains in the bay for a considerable time, with the potential adverse effects that this implies. The accident occurred at coordinates -5.42° longitude, 36.14° latitude and consisted of an oil spill of 48 h under calm wind. Oil properties are the same as above. It may be seen in Fig. 14 that after 12 days the patch is still in Algeciras Bay, its west coast being heavily contaminated. Some oil also reaches the east side of the bay (Gibraltar). Only winds from the north produce a faster cleaning of the bay.

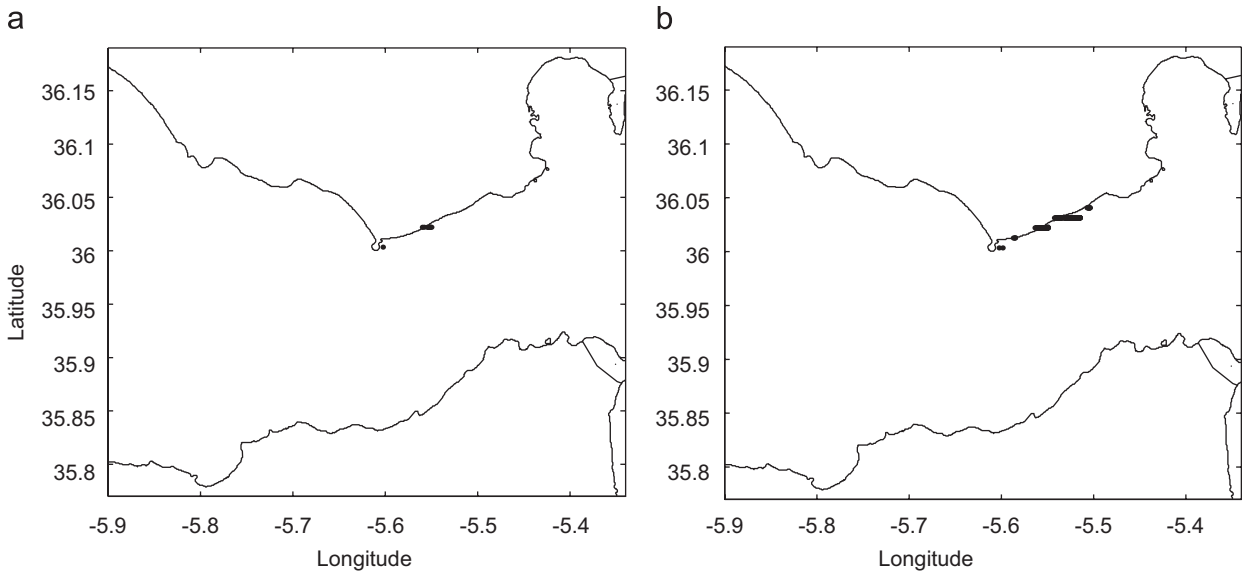

Fig. 13. Position of beached particles at 32 (a) and 48 (b) h after the oil spill in Fig. 12.

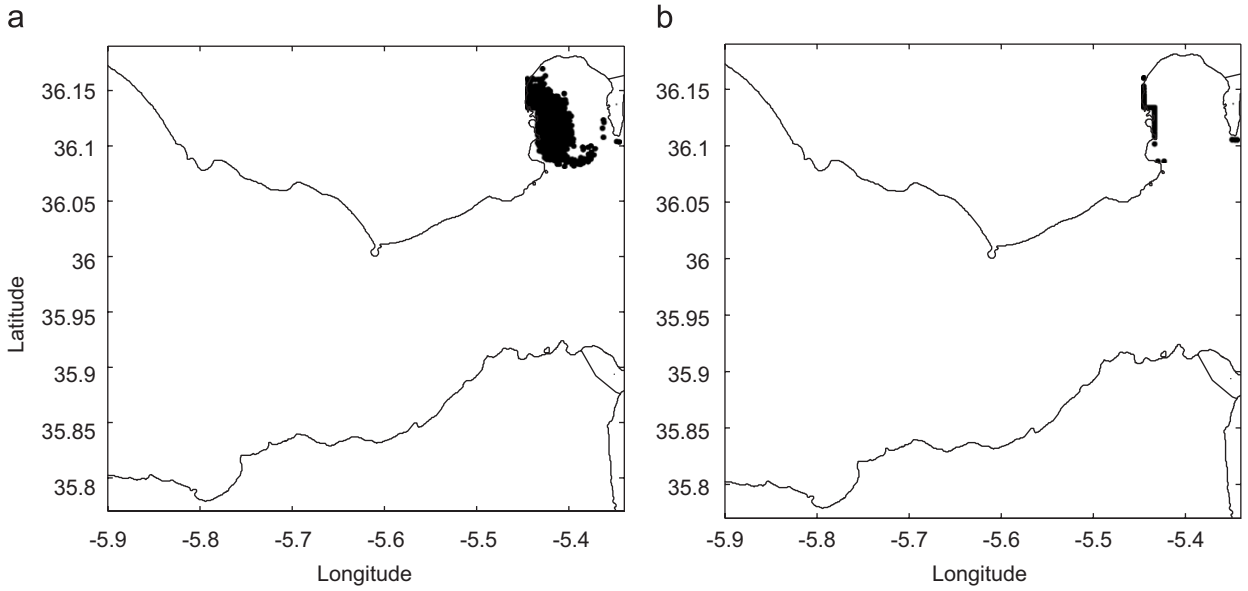

Fig. 14. Position of particles in water (a) and beached particles (b) 12 days after an accident close to Algeciras refinery.

4. Conclusions

A particle-tracking model that simulates the dispersion of chemical, radioactive and oil spills in Gibraltar Strait has been developed. The contamination release is simulated by a number of particles whose paths are computed. Diffusion is simulated by a Monte Carlo method. Specific processes for oil spills are also included: buoyancy, evaporation and beaching of oil droplets. The currents required to calculate the advective transport are obtained from a hydrodynamic model. Contaminant concentrations are obtained from the density of particles per water volume unit. A 2D barotropic model is used to calculate tidal currents over the domain. This model provides the tidal constants that are used by the dispersion model to reconstruct the tidal current at any time and position in the model domain. This

model has been validated through the comparison of computed tidal elevations, phases and currents with measurements in the area. Computed mean currents have also been compared with available data. Results are, in general, in good agreement with observations in the Strait. MatLab GUIs have been developed to allow easier model–user interactions.

Some dispersion calculations have been carried out as examples of model performance. In general, contaminants are flushed towards the east due to the mean current. Nevertheless, dominant east winds tend to retain contamination in the Strait and to enhance mixing. This is also the case if the release occurs close to the coast, where currents are weaker than in the central part of the Strait. The accident that implies the highest risk on local population would take place at, or near, Algeciras port. In this case contamination stays into Algeciras Bay. A faster flushing of contaminants out of the bay occurs only if wind blows from the north sector.

Generally speaking, this kind of dispersion model provides valuable information that may be used to support the decision-making process during an emergency situation arising from an accidental or deliberate release of contaminants in the marine environment.

Acknowledgment

This work was supported by the Research Project of Excellence RNM-419 Técnicas Ultrasensibles para la Determinación de Radionucleidos en Muestras Ambientales, Junta de Andalucía, Spain.

References

Candela, J., Winant, C., Ruiz, A., 1990. Tides in the Strait of Gibraltar. Journal of Geophysical Research 95, 7313–7335.

Delhez, E.J.M., 1996. On the residual advection of passive constituents. Journal of Marine Systems 8, 147–169.

Dick, S., Schonfeld, W., 1996. Water transport and mixing in the North Frisian Wadden Sea. Results of numerical investigations. German Journal of Hydrography 48, 27–48.

Echevarría, F., García-Lafuente, J., Bruno, M., Gorsky, G., Goutx, M., González, N., García, C.M., Gómez, F., Vargas, J.M., Picheral, M., Striby, L., Varela, M., Alonso, J.J., Reul, A., Cozar, A., Prieto, L., Sarhan, T., Plaza, F., Jiménez-Gómez, F., 2002. Physical–biological coupling in the Strait of Gibraltar. Deep-Sea Research II 49, 4115–4130.

Elliott, A.J., 1986. Shear diffusion and the spread of oil in the surface layers of the North Sea. German Journal of Hydrography 39, 113–137.

Elliott, A.J., 1999. Simulations of atmospheric dispersion following a spillage of petroleum at sea. Spill Science and Technology Bulletin 5, 39–50.

Elliott, A.J., 2004. A probabilistic description of the wind over Liverpool Bay with application to oil spill simulations. Estuarine Coastal and Shelf Science 61, 569–581.

Elliott, A.J., Wilkins, B.T., Mansfield, P., 2001. On the disposal of contaminated milk in coastal waters. Marine Pollution Bulletin 42, 927–934.

Flather, R.A., Heaps, N.S., 1975. Tidal computations for Morecambe Bay. Geophysical Journal of the Royal Astronomical Society 42, 489–517.

García-Lafuente, J., 1986. Variabilidad del nivel del mar en el estrecho de Gibraltar: mareas y oscilaciones residuales (Sea level variability in the Strait of Gibraltar: tides and residual oscillations). Ph.D. Dissertation, Instituto Español de Oceanografía, Málaga, Spain 154pp (in Spanish).

Gómez-Gesteira, M., Montero, P., Prego, R., Taboada, J.J., Leitao, P., Ruiz-Villareal, M., Neves, R., Perez-Villar, V., 1999. A two-dimensional particle-tracking model for pollution dispersion in A Coru na and Vigo Rias (NW Spain). Oceanologica Acta 22, 167–177.

Harms, I.H., Karcher, M.J., Dethleff, D., 2000. Modelling Siberian river runoff—implications for contaminant transport in the Arctic Ocean. Journal of Marine Systems 27, 95–115.

Jensen, T.G., 1998. Open boundary conditions in stratified ocean models. Journal of Marine Systems 16, 297–322.

Korotenko, K.A., Mamedov, R.M., Kontar, A.E., Korotenko, L.A., 2004. Particle-tracking method in the approach for prediction of oil slick transport in the sea: modelling oil pollution resulting from river input. Journal of Marine Systems 48, 159–170.

León-Vintró, L., Mitchell, P.I., Condren, O.M., Downes, A.B., Papucci, C., Delfanti, R., 1999. Vertical and horizontal fluxes of plutonium and americium in the western Mediterranean and the Strait of Gibraltar. The Science of the Total Environment 237, 77–91.

Mañanes, R., Bruno, M., Alonso, J., Fraguela, B., Tejedor, L., 1998. Non-linear interaction between tidal and subinertial barotropic flows in the Strait of Gibraltar. Oceanologica Acta 21, 33–46.

Nakano, M., Povinec, P., 2003. Oceanic general circulation model for the assessment of the distribution of ^{137}Cs in the world ocean. Deep-Sea Research II 50, 2803–2816.

Periáñez, R., 2005a. An operative lagrangian model for simulating radioactivity dispersion in the Strait of Gibraltar. Journal of Environmental Radioactivity 84, 95–101.

Periáñez, R., 2005b. Modelling the Dispersion of Radionuclides in the Marine Environment. Springer, Heidelberg, 201pp.

Periáñez, R., 2006. Modelling surface radioactive spill dispersion in the Alborán Sea. Journal of Environmental Radioactivity 90, 48–67.

Periáñez, R., Elliott, A.J., 2002. A particle tracking method for simulating the dispersion of non-conservative radionuclides in coastal waters. Journal of Environmental Radioactivity 58, 13–33.

Proctor, R., Flather, R.A., Elliott, A.J., 1994a. Modelling tides and surface drift in the Arabian Gulf: application to the Gulf oil spill. Continental Shelf Research 14, 531–545.

Proctor, R., Elliott, A.J., Flather, R.A., 1994b. Forecast and hindcast simulations of the Braer oil spill. Marine Pollution Bulletin 28, 219–229.

Pugh, D.T., 1987. Tides, Surges and Mean Sea Level. Wiley, Chichester, UK, 472pp.

Riddle, A.M., 1998. The specification of mixing in random walk models for dispersion in the sea. Continental Shelf Research 18, 441–456.

Sannino, G., Bargagli, A., Artale, V., 2004. Numerical modelling of semidiurnal tidal exchange through the Strait of Gibraltar. Journal of Geophysical Research 109, C05011.

Schonfeld, W., 1995. Numerical simulation of the dispersion of artificial radionuclides in the English Channel and the North Sea. Journal of Marine Systems 6, 529–544.

Stentchev, A., Korotenko, K., 2005. Dispersion processes and transport pattern in the ROFI system of the eastern English Channel derived from a particle-tracking model. Journal of Marine Systems 25, 2294–2304.

Tejedor, L., Izquierdo, A., Kagan, B.A., Sein, D.V., 1999. Simulation of the semidiurnal tides in the Strait of Gibraltar. Journal of Geophysical Research 104, 13541–13557.

Tsimplis, M.N., Bryden, H.L., 2000. Estimations of the transports through the Strait of Gibraltar. Deep-Sea Research 47, 2219–2242.

Tsimplis, M.N., Proctor, R., Flather, R.A., 1995. A two dimensional tidal model for the Mediterranean Sea. Journal of Geophysical Research 100, 16223–16239.